1.14-GHz Self-Aligned Vibrating Micromechanical Disk Resonator

Jing Wang, Zeying Ren, and Clark T.-C. Nguyen

Center for Wireless Integrated Microsystems (WIMS), Dept. of Electrical Engineering and Computer Science, University of Michigan, Ann Arbor, Michigan 48109-2122 USA

Abstract—**Micromechanical radial-contour mode disk resonators featuring new self-aligned stems have been demonstrated with record resonance frequencies up to 1.14 GHz and measured *Q*'s at this frequency >1,500 in *both vacuum and air*. In addition, a 733-MHz version has been demonstrated with *Q*'s of 7,330 and 6,100 in vacuum and air, respectively. For these resonators, self-alignment of the stem to exactly the center of the disk it supports allows balancing of the resonator far superior to that achieved by previous versions (where separate masks were used to define the disk and stem), allowing the present devices to retain high *Q* while achieving frequencies in the GHz range for the first time. In addition to providing measured results, this paper formulates an equivalent electrical circuit model that accurately predicts the performance of this disk resonator.**

Index Terms—**microelectromechanical devices, MEMS, resonator, RF, quality factor**

I. Introduction

Vibrating micromechanical ("μmechanical") resonators are emerging as viable candidates for on-chip versions of the high-*Q* resonators (e.g, quartz crystals, SAW resonators) used in wireless communication systems [1] for frequency generation and filtering. However, although micro-scale versions have reached frequencies up to the mid-VHF range (156 MHz [2]) with *Q*'s approaching 10,000, the acceptance of such devices in present-day communication transceivers has so far been hindered by several remaining issues, including: (1) a frequency range that had not surpassed 1 GHz; (2) the need for vacuum to attain high *Q*; and (3) higher impedances than normally presented by macroscopic high-*Q* resonators.

This work now alleviates the first two of the above issues. In particular, micromechanical radial-contour mode vibrating disk resonators featuring new self-aligned stems have been demonstrated with record resonance frequencies up to 1.14 GHz and measured *Q*'s at this frequency >1,500 in *both vacuum and air*. In addition, a 733-MHz version has been demonstrated with *Q*'s of 7,330 and 6,100 in vacuum and air, respectively. For these resonators, self-alignment of the stem to exactly the center of the disk it supports allows symmetrical balancing of the resonator far superior to that achieved by previous versions (where separate masks were used to define the disk and stem), allowing the present devices to retain high *Q* while achieving frequencies in the GHz range for the first time.

In addition to describing the design, operation, and fabrication of self-aligned disk resonators, this paper formulates an equivalent circuit model for these devices, then verifies it with measurements on fabricated disks.

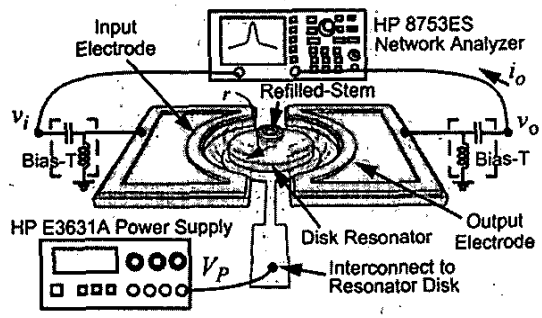

Fig. 1: Perspective-view schematic of a self-aligned disk resonator identifying key features and a two port measurement scheme.

II. Device Structure, Operation, and Modeling

Figure 1 presents the perspective-view schematic of a self-aligned disk resonator identifying key features, and illustrating a typical two-port bias, excitation, and measurement scheme. As shown, this device consists of a 2μm-thick polysilicon disk suspended by a 2μm-diameter stem self-aligned to its center and enclosed by two polysilicon electrodes spaced less than 1,000Å from the disk perimeter. In the schematic, the tops of the electrodes have been rendered transparent to enable viewing of the underlying structure.

The dimensions needed to attain a specified resonance frequency f_o for a radial-contour mode disk can be obtained by solving the mode frequency equation, given by [3]

$$\delta \times \frac{J_0(\delta)}{J_1(\delta)} = 1 - \sigma \qquad (1)$$

where

$$\delta = \omega_o R \sqrt{\frac{\rho(1-\sigma^2)}{E}}, \qquad (2)$$

and where R is the disk radius; $\omega_o = 2\pi f_o$ is the angular resonance frequency; $J_n(y)$ is the Bessel function of the first kind of order n; ρ, σ, and E are the density, Poisson ratio, and Young's modulus, respectively, of the structural material.

To excite the device of Fig. 1 in its two-port configuration, a dc-bias voltage V_P is applied to the disk and an ac signal v_i to its input electrode, generating an input force F_i in a radial direction (pointing outward from the disk) at the frequency of v_i given by

$$F_i = -V_P \left(\frac{\partial C}{\partial r}\right)_i v_i \qquad (3)$$

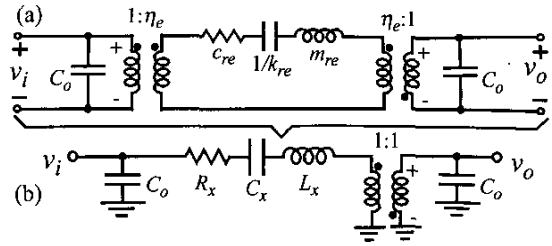

Fig. 2: Equivalent circuit models for a two-port disk resonator. (a) Physically consistent model using actual values of mass and stiffness for elements. (b) Purely electrical model.

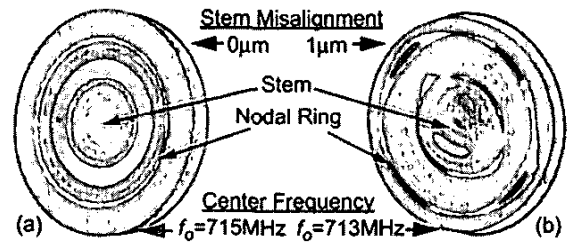

Fig. 3: ANSYS modal displacement simulation for a 20μm-diameter, 2μm-stem, radial-contour mode disk for the cases of (a) perfectly centered stem; and (b) a stem offset from the center by only 1μm.

where $(\partial C/\partial r)_i$ is the integrated change in electrode-to-resonator overlap capacitance per unit radial displacement at the input (drive) port. When the frequency of v_i matches the radial-contour mode resonance frequency of the disk, the resulting force drives the disk into a vibration mode shape where it expands and contracts radially around its perimeter, in a fashion reminiscent of "breathing". This motion creates a time-varying capacitance between the disk and output electrode, which if the electrode is shunted to ground, results in an output current given by

$$i_o = V_P\left(\frac{\partial C}{\partial r}\right)_o \frac{\partial r}{\partial t} = -\omega_o \frac{Q}{k_{re}}\left(\frac{\partial C}{\partial r}\right)_i \left(\frac{\partial C}{\partial r}\right)_o V_P^2 v_i \qquad (4)$$

where $(\partial C/\partial r)_o$ is the change in electrode-to-resonator overlap capacitance per unit radial displacement at the output port. In effect, this device operates by first converting the input electrical signal v_i to a mechanical force F_i, which gets filtered by the high-Q mechanical response of the resonator, allowing only components at the disk resonance frequency to be converted to a disk displacement r (or velocity v). This mechanical domain displacement r is then converted back to the electrical domain into the output current i_o by action of the output electrode capacitive transducer.

Despite its mechanical nature, the disk resonator of Fig. 1 still looks like an electrical device when looking into its ports, and so can be modeled by either of the electrical *LCR* equivalent circuits shown in Fig. 2. The element values for the *LCR* equivalent to the radial-contour mode disk is governed by the total integrated kinetic energy in the resonator, its mode shape, and parameters associated with its transducer ports [4]. Using the procedure of [5] for symmetrical electrodes, the expressions for equivalent inductance L_x, capacitance C_x, and series motional resistance R_x in the purely electrical version of the *LCR* can be written as

$$L_x = \frac{m_{re}}{\eta_e^2} \qquad C_x = \frac{\eta_e^2}{\omega_o^2 m_{re}} \qquad R_x = \frac{\omega_o m_{re}}{Q\,\eta_e^2} \qquad (5)$$

where

$$m_{re} = \frac{2\pi\rho t\int_0^R rJ_1^2(hr)dr}{J_1^2(hR)}, \; h = \sqrt{\frac{\omega_o^2\rho}{\left(\frac{2E}{2+2\sigma}+\frac{E\sigma}{1-\sigma^2}\right)}} \qquad (6)$$

$$\eta_e = V_P\left(\frac{\partial C}{\partial r}\right), \; k_{re} = \omega_o^2 m_{re} \qquad (7)$$

and where m_{re} and k_{re} are the effective equivalent mass and stiffness, respectively, of the disk in its radial-contour mode, and t is thickness.

The C_o in each circuit of Fig. 2 represents capacitance from an I/O electrode to ac ground, and as such, is primarily composed of a combination of electrode-to-resonator overlap capacitance and electrode-to-substrate capacitance.

One important difference between the stiff, high frequency resonators of this work and previous lower frequency ones is the difference in total energy per cycle. In particular, the peak kinetic energy per cycle can be computed via the expression

$$KE_{peak} = \frac{1}{2}m_{re}(\omega_o X)^2 = \frac{1}{2}k_{re}X^2, \qquad (8)$$

where X and k_{re} are the peak displacement and effective stiffness, respectively, at the disk location across from the center of an electrode. Given that the k_{re} ~73.5 MN/m for a 1.14-GHz disk resonator is more than 49,000X the 1,500 N/m of a 10-MHz CC-beam, the former is expected to store 49,000X more energy per cycle for the same displacement amplitude. With energies per cycle many times larger than those lost to viscous gas damping, the resonators of this work, and virtually any high stiffness, high frequency μmechanical resonator device, are expected to exhibit high Q even under air damped conditions.

III. Self-Aligned Stem Fabrication Process

As mentioned, the key feature of this work that allows radial contour mode disk resonators to achieve frequencies >1 GHz with exceptional Q is the use of a new fabrication technology that allows self-alignment (i.e., exact placement) of the stem at the center of the disk. To illustrate the importance of perfect alignment, Fig. 3 presents ANSYS modal displacement analyses on a radial-contour mode disk for the cases of (a) a perfectly centered stem; and (b) a stem offset from the center by only 1 μm. Here, a perfectly centered stem leads to a symmetric and purely radial 2nd contour mode shape. Conversely, even just 1 μm of misalignment leads to dramatic mode shape distortions and consequent acoustic energy losses to the substrate that lower the Q, making resonance detection difficult.

Figure 4 presents cross-sections summarizing the process flow that achieves self-aligned stems. The process begins with polysilicon surface micromachining steps similar to

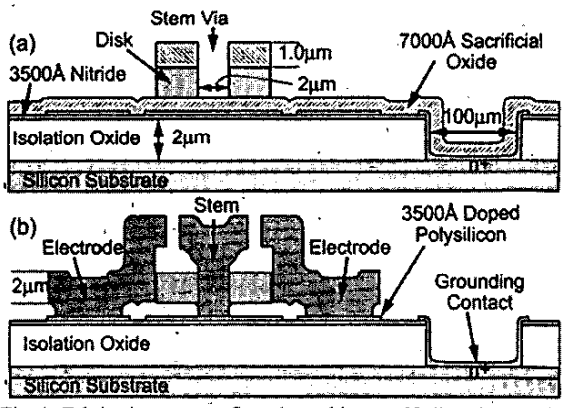

Fig. 4: Fabrication process flow that achieves self-aligned stems for radial-contour mode disk resonators, and includes a substrate ground plane to suppress parasitic feedthrough.

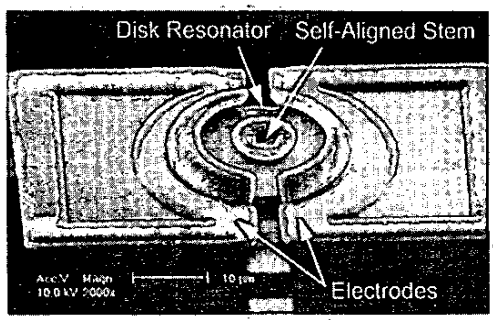

Fig. 5: SEM of a 20μm-diameter radial-contour mode disk resonator with self-aligned stem fabricated by the process of Fig 4.

those used in a previous metal electrode small-gap process [6] up to the point of defining the disk structure. The process then deviates from [6] with an etch step that patterns not only the disk and support structures, but also vias for any anchors to be formed, yielding the cross-section shown in Fig. 4(a). A sidewall sacrificial oxide spacer is then deposited to define the electrode-to-resonator gap, as in [6], but additional steps are taken to remove this sidewall sacrificial layer in the anchor vias, then to etch through the bottom sacrificial layer down to the substrate. With exposed anchor vias, a subsequent (third) polysilicon deposition then not only provides the material for electrodes, but also refills the anchor vias to create very rigid, self-aligned anchors. This third polysilicon layer is then $POCl_3$-doped and patterned to delineate the electrodes, after which an HF release etch achieves the final cross-section of Fig. 4(b).

Figure 5 presents the SEM of the 20μm-diameter self-aligned μmechanical disk resonator fabricated using the process of Fig. 4 and used for all measurements to follow.

IV. Experimental Results

As mentioned in the introduction, micromechanical resonators often exhibit port-to-port impedances much larger than conventional macroscopic devices. Although not perceived to be as much of a problem when the resonators are

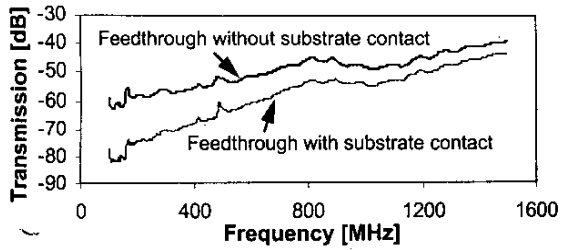

Fig. 6: Measured feedthrough vs. frequency for devices with and without a substrate contact.

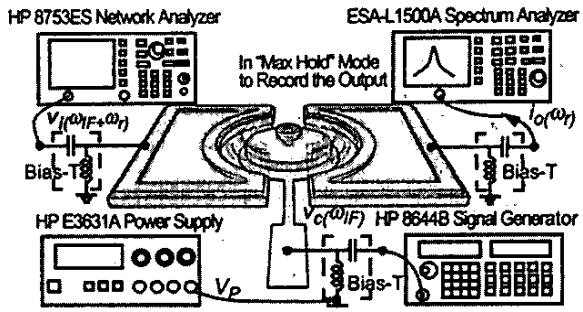

Fig. 7: Perspective-view schematic of a self-aligned disk resonator illustrating, mixing measurement scheme an key instruments used.

utilized in single-chip, fully integrated systems, where the resonators are integrated directly alongside transistors, difficulties can arise when these devices must interface directly with off-chip, macroscopic components, such as 50Ω measurement instrumentation.

In most cases, despite large impedance mismatching, a direct two-port measurement set-up, such as shown in Fig. 1, was sufficient to obtain frequency and Q data, albeit with up to ~62 dB of transmission loss caused not by the resonator device, but by the large mismatch between the resonator impedance and the 50Ω network analyzer test-port impedance. The use of a contactable substrate ground plane to shunt feedthrough currents away from the output electrode proved instrumental in allowing direct two-port measurement of devices. As shown in the measured feedthrough vs. frequency plots of Fig. 6, more than 10dB of feedthrough suppression was achieved at frequencies below 1 GHz via substrate grounding.

For cases where impedance-mismatches made direct two-port measurement impossible, despite substrate grounding, a mixing-based measurement set-up shown in Fig. 7 was used that suppressed parasitic feedthrough by moving motional currents away from them in the frequency domain [7], allowing adequate measurement of devices. In either case, it should be noted that losses seen in the measured spectra to follow arise from impedance mismatching, and are not indicative of device loss. By their sheer high Q, it should be obvious that the devices should exhibit very little loss when used in properly matched filters [4].

Figures 8 and 9 present frequency spectra measured using the mixing set-up of Fig. 7 for the device of Fig. 5 operating in its second radial contour mode at 733 MIIz, with a Q of

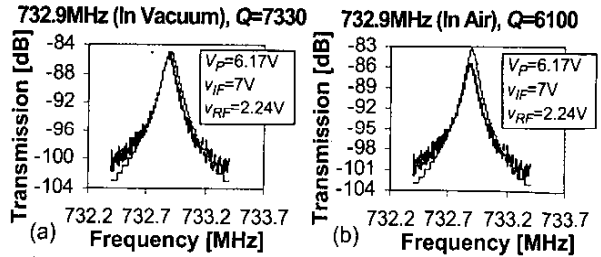

Fig. 8: Measured (dark) and predicted (light) frequency characteristics for a 733-MHz, 2nd mode, 20μm-diameter disk resonator measured in (a) vacuum and (b) in air, using the setup shown in Fig. 7.

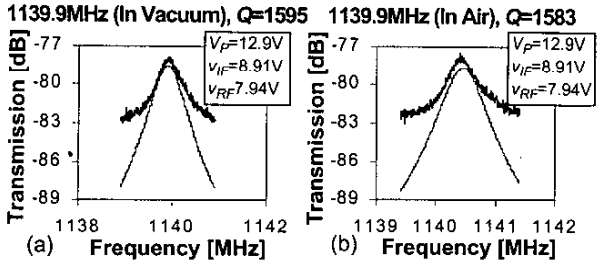

Fig. 9: Measured (dark) and predicted (light) frequency characteristics for a 1.14-GHz, 3rd mode, 20μm-diameter disk resonator measured in (a) vacuum and (b) in air, using the setup shown in Fig. 7.

Table I: Simulated vs. Measured *RLC* Values

Freq. [MHz]	732.9	732.9	733	1140	1140	1140
Meas/Calc	Meas	Calc	Calc	Meas	Calc	Calc
Q	7330	7330	7330	1600	1600	1600
V_P [V]	6.17	6.17	100	12.9	12.9	100
Gap, d [A]	860	860	550	740	740	550
Thickness, t [μm]	2.1	2.1	10.0	2.1	2.1	10.0
R_x [kΩ]	3772	3891	0.520	3456	3546	3.781
L_x [mH]	6005	6194	8.28	792	772	8.45
C_x [10^{-20}F]	0.785	0.761	5691	2.46	2.52	2308

7,330 in vacuum and 6,100 in air; and in its third radial contour mode at 1.14 GHz with Q's of 1,595 and 1,583, in vacuum and air, respectively. (It should be noted that due to impedance mismatching, the peak height in the latter measurement is quite small, so the extracted Q probably undershoots the actual value by a significant amount.) Both measurements verify the prediction of Section II that the Q's of high stiffness, high frequency devices should remain high whether operated in vacuum or at atmospheric pressure. In addition to measured spectra, theoretical curves predicted using the formulations of Section II are included in the plots, verifying the accuracy of the models. Table I further presents a comparison of measured and predicted equivalent circuit element values, showing very good agreement.

To attain smaller resistances, higher DC bias and smaller electrode-to-resonator gaps are needed. In particular, the use of a 30.54V DC bias voltage yields a measured R_x at 737.4 MHz of 58.072 kΩ, which compares well with the 64.585 kΩ predicted by (5), further attesting to its accuracy. In addition, (5) predicts R_x's on the order of 520Ω with a DC-bias of 100V, a resonator disk thickness of 10μm, and an electrode-to-resonator gap spacing of 550Å. Although 100V seems excessive, it is not entirely unreasonable when one considers that it emanates from a charge placed on the resonator, where no current is flowing, hence no power is consumed. Still, smaller DC bias voltages are preferred, so research on resonator arrays [8] and alternative resonator designs to lower the required DC bias voltage is ongoing.

V. Conclusions

By eliminating anchor-to-disk misalignment error through self-alignment, the radial contour mode polysilicon micromechanical disk resonators of this work have now achieved frequencies in excess of 1 GHz with Q's still >1,500. In addition, given that the 733-MHz disk achieved a frequency-Q product of 5.37×10^{12}, which is similar to that of a previous lower frequency (VHF) polysilicon resonator [9], there is evidence that the Q of 1,595 measured for the 1.14-GHz device undershoots the actual value. In particular, even with the conservative assumption that Q might roll off linearly with frequency, this f_o-Q product suggests that the Q's of 5,400 at 1 GHz are not unreasonable. Furthermore, these high stiffness, high frequency devices attain almost the same high Q values whether operated in vacuum or air. The implications here are enormous, as this result effectively states that vacuum is no longer needed to attain exceptional Q in high frequency vibrating micromechanical resonators—a fact that should substantially lower the cost of devices based on vibrating RF MEMS technology, making them strong contenders in numerous wireless communication applications, provided impedance matching issues can be alleviated. Research to address impedance matching issues at both the device and system levels is ongoing.

Acknowledgment. This work was supported by DARPA and an NSF ERC in Wireless Integrated Microsystems.

References

[1] C. T.-C. Nguyen, *Dig. of Papers*, Topical Mtg on Silicon Monolithic IC's in RF Systems, Sept. 12-14, 2001, pp. 23-32.

[2] J. R. Clark, *et al.*, *Tech. Digest*, IEEE Int. Electron Devices Meeting, Dec. 11-13, 2000, pp. 399-402.

[3] M. Onoe, *J. Acoustic. Soc. Amer.*, pp1158-1162, Nov. 1956.

[4] R. A. Johnson, *Mechanical Filters in Electronics*. New York, NY: Wiley, 1983.

[5] F. D. Bannon III, *et al.*, *IEEE J. Solid-State Circuits*, vol. 35, no. 4, pp. 512-526, April 2000.

[6] W.-T. Hsu, *et al.*, *Tech. Digest*, IEEE Int. Micro Electro Mechanical Systems Conf., Jan. 21-25, 2001, pp.349-352.

[7] Ark-chew Wong, *et al.*, *Tech. Digest*, IEEE Int. Electron Devices Meeting, Dec. 6-9, 1998, pp. 471-474.

[8] M. Demirci, *et al.*, to be published in the *Tech. Digest* of Transducers'03, Boston, MA, June 8-12, 2003.

[9] M. Abdelmoneum, *et al.*, *Tech. Digest*, IEEE Int. Micro Electro Mechanical Systems Conf., Jan. 19-23, 2003, pp. 698-701.